LA-UR- 96- 4894

Approved for public release; distribution is unlimited.

Title: SURFACE WATER AND EROSION CALCULATIONS TO SUPPORT THE MDA G PERFORMANCE ASSESSMENT

LA-UR--96-4894

Author(s): E. P. Springer, EES-15

Submitted to: Los Alamos Report

MASTER

DISCLAIMER

Los Alamos
NATIONAL LABORATORY

DISTRIBUTION OF THIS DOCUMENT IS UNLIMITED

SURFACE WATER AND EROSION CALCULATIONS TO SUPPORT THE MDA G PERFORMANCE ASSESSMENT

E. P. Springer

INTRODUCTION

The performance of MDA G is dependent on surface hydrological and ecological processes because radionuclide transport by surface runoff can affect human and/or environmental receptors directly and the percolation for the subsurface radionuclide transport pathway is determined by the water balance in the near surface. For subsurface disposal of waste, surface soil erosion reduces the effectiveness of the surface cover and if wastes are exposed, then surface runoff can transport contaminants either in a soluble phase or sorbed to eroded soil particles. The objectives of this section are to estimate the effects at MDA G of surface runoff, soil erosion, and percolation. The conceptual and mathematical models will be reviewed, parameter estimation for the models will be presented and results and sensitivity analyses for a surface cover at MDA G will be presented.

CONCEPTUAL MODEL

Water Balance

The basic conceptual model that governs the surface water pathway is the water balance equation written as

$$\frac{dS}{dt} = P - Q - ET - R \qquad (1)$$

where:
S = soil water storage (mm);
P = precipitation (mm);
Q = surface runoff (mm);
ET = evapotranspiration (mm);
R = the deep percolation (mm); and
t = time.

Equation 1 is used to describe the water balance for conceptual cover at disposal pit at MDA G. Precipitation may be either rain or snow. Evapotranspiration is from both soil evaporation and plant transpiration. Deep percolation is defined as that water draining below the pit. Figure 1 presents the conceptual model represented by Equation 1.

One key assumption for this application of Equation 1 to MDA G is that the cover is topsoil over crushed tuff. Cover designs can include a low permeability layer such as clay (Warren et al., 1996) or a capillary barrier (Nyhan et al., 1990) to divert infiltrated water. No credit was taken in the following analyses for any engineered cover design. The model is one-dimensional considering only the vertical coordinate.

Equation 1 is solved by measuring its various terms in field experiments. The following material reviews studies pertinent to the terms in Equation 1 that have been performed at or near MDA G to support the conceptual and mathematical models.

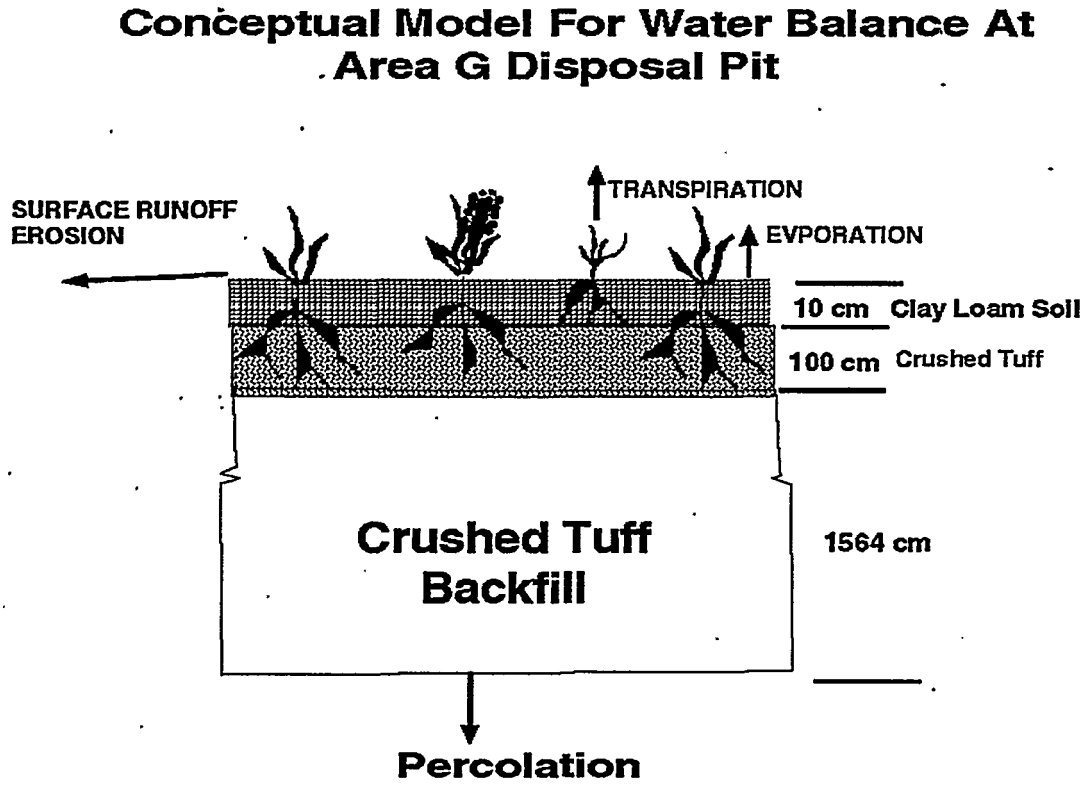

Figure 1. Conceptualization of hypothetical pit at MDA G for surface runoff and erosion assessment.

The focus of the following analyses is surface runoff (Q). Limited measurements of Q have been made for MDA G. Abeele et al. (1981) presented results (for a single event) from a runoff gauging station located at MDA G. Nyhan and Lane (1986b) used rainfall simulation to study surface runoff and soil erosion from different surface cover materials such as gravel mulch and vegetation at Los Alamos. Runoff data are available for one year for MDA G and the major canyons (Pajarito Canyon and Cañada del Buey) that drain the site as part of the Los Alamos stormwater quality program.

Soil moisture measurements have been made for various studies at MDA G. Results of a study by Purtyman are reported in Rogers (1977) for surface covers at Pits 1 and 2 in MDA G. These moisture data are presented in Figures 2 and 3. Note that the water content in Pit 1 is higher than Pit 2. The cause of this difference is unknown. Nyhan et al. (1986) performed a study at MDA G on Pit 25 using four different surface cover designs. One cover design includes the topsoil over crushed tuff like the cover design presented in Figure 1 that was used in this Performance Assessment. The other three cover designs had a biobarrier composed of a layer of either large cobbles or gravel and cobble to prevent plant and animal intrusion. Beneath each cover design, a layer of crushed tuff was placed, and the soil water content was measured in this layer. The temporal distribution of water content in this crushed tuff layer for the different cap configurations is presented Figure 4 which is from Nyhan et al. (1986). Generally, an increase in water content of the tuff layer can be observed for all cover designs early in 1983. A trend of decreasing water content occurs over the rest of 1983 followed by an increase in water content early in 1984 that is coincident with snowmelt period. Data in Figure 4 indicate that water can penetrate to depths greater than 1 meter. Nyhan et al. (1986) examined root penetration of the different designs using a cesium tracer placed in the crushed tuff layer beneath the cover designs. Substantial penetration was observed for the soil over tuff design providing a mechanism for water removal. Some root penetration was noted for the biobarrier designs, but this was not as prevalent as on the conventional design.

Nyhan et al. (1990) reported on a study of conventional and engineered surface covers at TA-51 located approximately 2 km west of MDA G. The conventional design consisted of loam soil over crushed tuff. The engineered design included a capillary barrier of pea gravel beneath the loam top soil and a biobarrier made of large cobble beneath the capillary barrier. The surface slope of these plots was zero in order to maximize infiltration: therefore no runoff occurred. Table 1 (Nyhan et al., 1990) gives the different components of the water balance for the two plot designs. These results indicate the relative distribution of the components in Equation 1 early in the performance period of these surface cap designs. Nyhan et al. (1990) attributed the seepage in the March to April period to snowmelt and low evapotranspiration demand because the vegetation was still dormant at this time of the year.

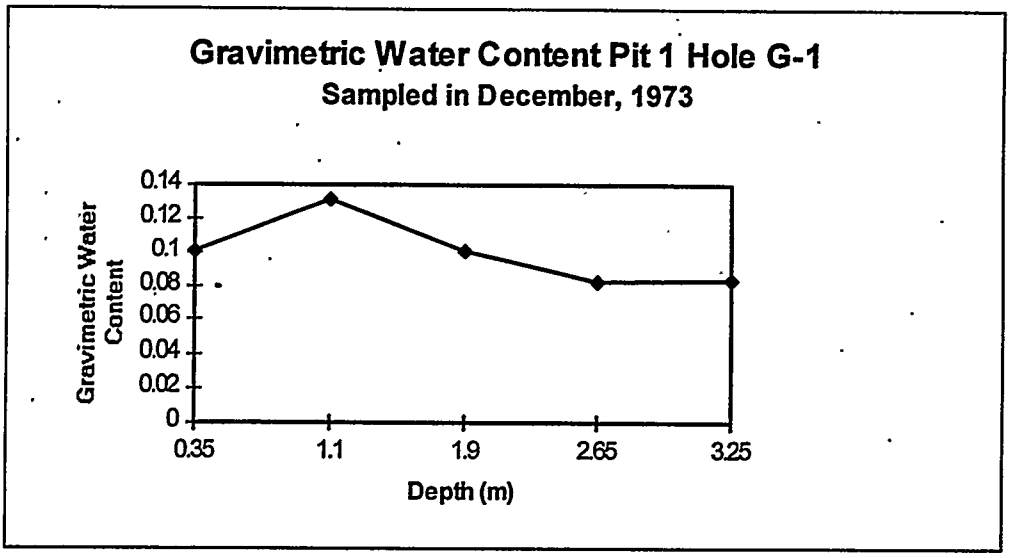

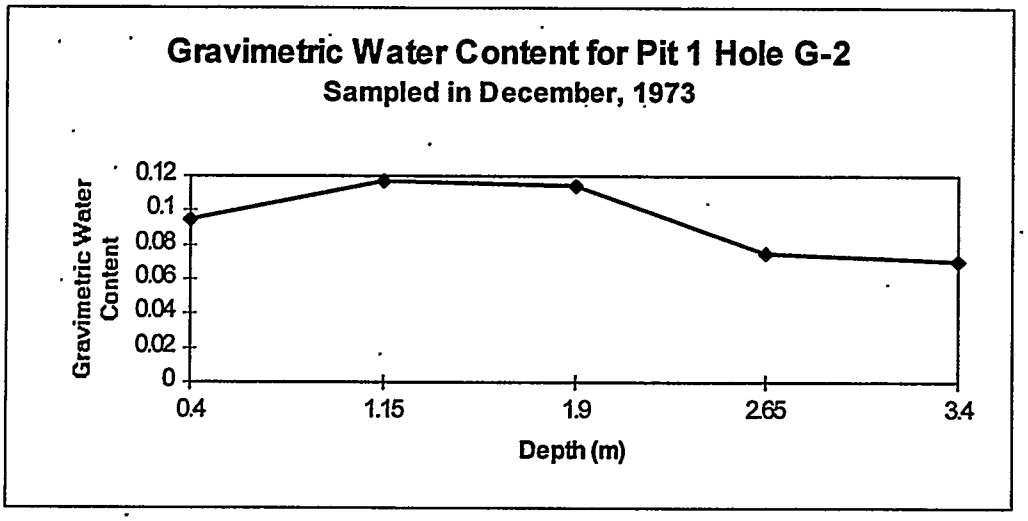

Figure 2. Gravimetric soil water content from two boreholes drilled in cover of MDA G pit number 1.

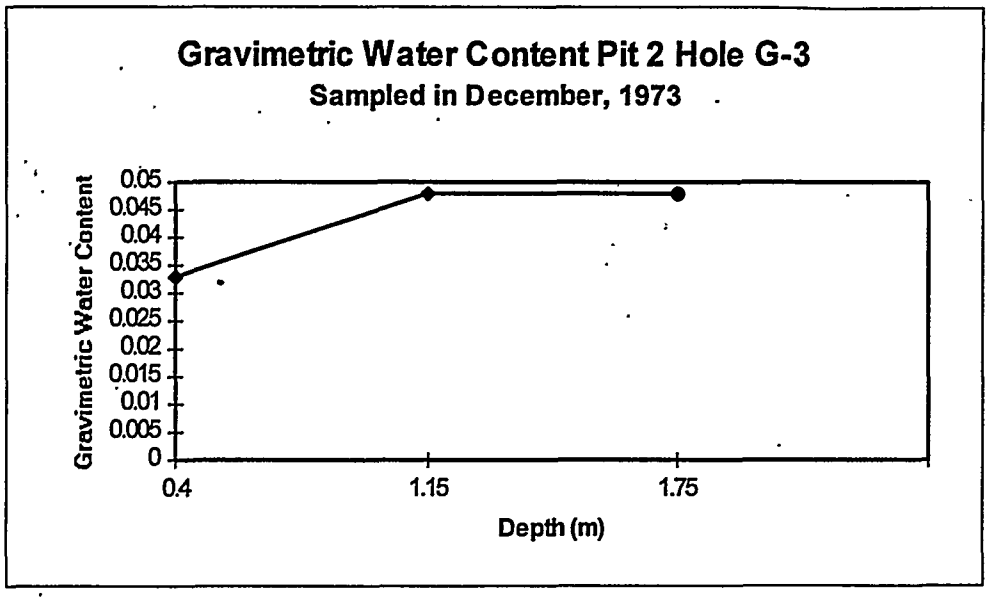

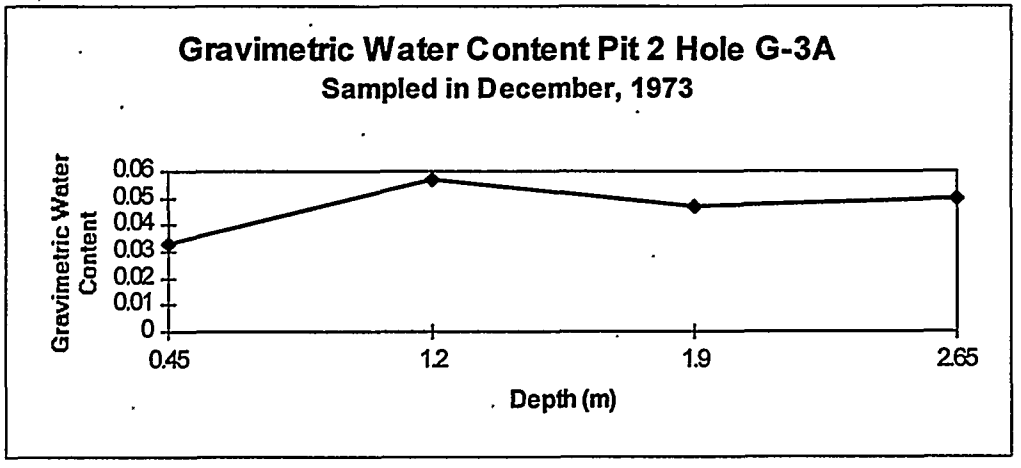

Figure 3. Gravimetric soil water content from two boreholes drilled in cover of MDA G Pit number 2.

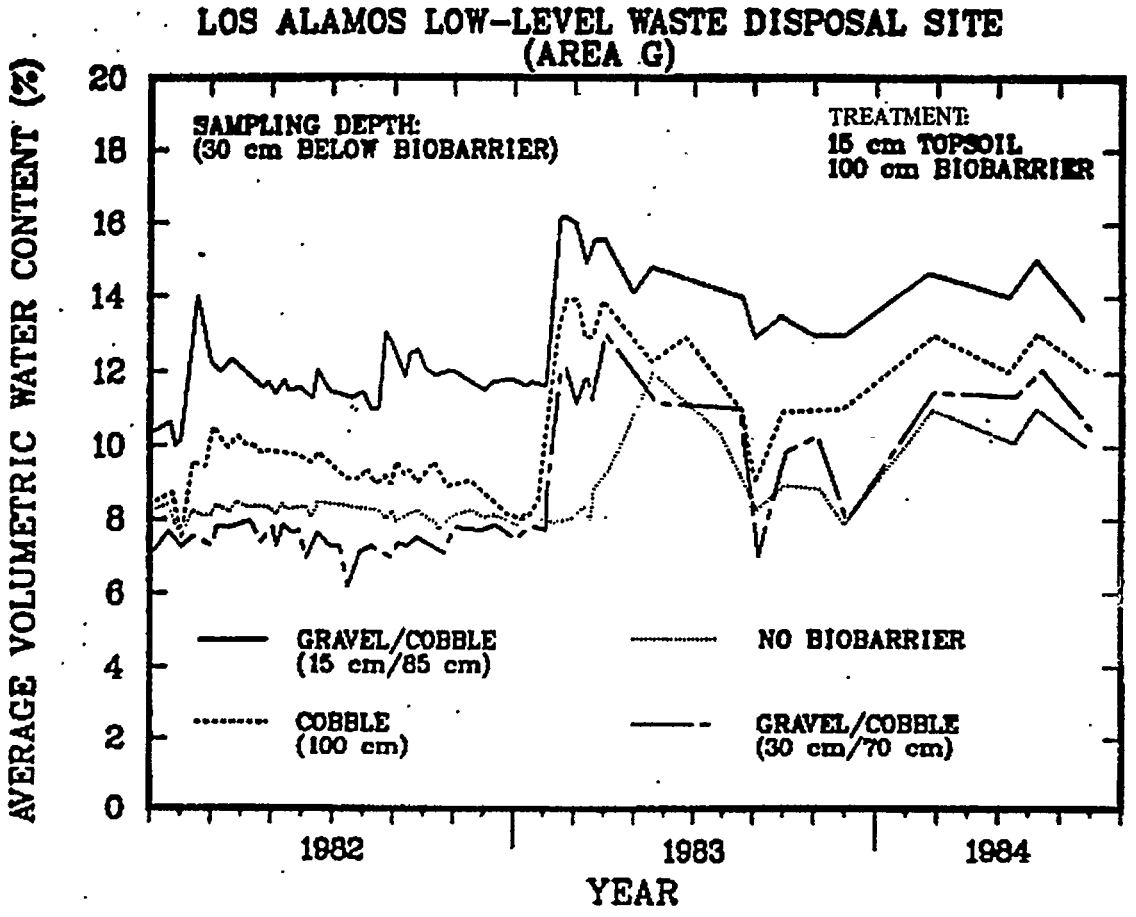

Figure 4. Volumetric water content in crushed tuff layer (137-cm sampling depth) beneath surface covers at MDA G (from Nyhan et al. 1986).

Table 1. Soil water balance components for cover experiment at TA-51 from Nyhan et al. (1990).

	Control Plots		Improved Plots	
	1	2	1	2
Precipitation (cm)	173.72	173.72	173.72	173.72
Soil water increase (cm)	12.09	9.09	4.15	4.43
Interflow (cm)	0	0	0	1.93
Percolation (cm)	10.62	10.63	0	2.64
Evapotranspiration	151.67	154.87	169.57	164.71

The available data suggest that water will penetrate a depth greater than 1 m at MDA G which is the cover thickness assummed in the performance assessment simulations. As vegetation is established, deeper rooted plants can remove moisture from deeper in the profile reducing the percolation. On the negative side, plant root uptake may become a pathway for radionuclides, and dead roots can provide channels for flow.

Soil Erosion

Soil erosion is defined for this problem as the removal of surface material by water. Wind is another agent that can remove surface material, but it is not included here. Soil erosion is included because the removal of surface soil will reduce cap thickness and may eventually expose wastes and because radionuclides adsorbed to soil particles can be transported.

Soil erosion studies on surface covers at Los Alamos were reported by Nyhan et al. (1984) and Nyhan and Lane (1986a). These studies used rainfall simulation technology with plots prepared for different surface cover schemes to determine parameters for the Universal Soil Loss Equation (USLE) (Wischmeier and Smith, 1978). As expected soil erosion was greatest on plots that were recently disturbed and had little or no cover. The soil loss measured by Nyhan et al. (1984) from the natural plots was 2% of that from cultivated plots. Nyhan and Lane (1986a) showed an order of magnitude reduction in the USLE cover management (C) factor when a 70% gravel mulch surface cover was applied compared to the bare soil surface cover. A further factor of two reduction in soil loss was suggested when a vegetation was used in conjunction with the gravel mulch but these results were highly variable. Data from these studies were used by Nyhan and Lane (1986b) to determine parameters for the USLE to apply to shallow land burial sites at Los Alamos.

Soil erosion is a function of soil properties, surface conditions, topography, climate, and land management. The Universal Soil Loss Equation (USLE) uses a multiplicative

expression to relate these factors (Wischmeier and Smith, 1978; Nyhan and Lane, 1986b). The USLE estimates long-term average annual soil loss for a site using a climate factor. For the Performance Assessment, the Modified Universal Soil Loss Equation (MUSLE) was used because daily hydrologic information was available (Williams, 1975).

Biological Intrusion

Intrusion into surface covers by animals and vegetation has important implications for surface runoff and erosion. Intrusion can have positive and negative effects on surface cover performance. Suter et al. (1993) reviewed the effects that vegetation and burrowing animals may have on surface covers. For vegetation, the most detrimental effects are penetrating hydrologic barriers thus reducing their effectiveness, and root uptake of waste material. Vegetation is needed to reduce potential percolation of water and minimize water and wind erosion. Burrowing animals can provide a more direct route for water to the waste, and if the animals penetrate the waste burrowing animals can move contaminated soil or waste to the surface where it can be eroded.

Studies from many different locations were reviewed by Suter et al. (1993). Link et al. (1995) summarized information on vegetation and animal effects for Hanford which is a semiarid site like Los Alamos. Their studies concluded that small mammal burrows have little or no effect on soil moisture content. They cautioned that this result was based on short-term studies.

Sejkora and Alldredge (1989) used rainfall simulation to study the influence of pocket gophers on runoff and erosion. Runoff and soil loss were measured on bare and vegetated plots with and without gophers. The results indicated that introducing gophers reduced runoff by an average of 21% and soil loss by 42% after four weeks of activity by the gophers in the plots. The authors concluded from this short-term study that cumulative impacts of the gophers will increase with time and that the presence of the gophers may affect other factors such as vegetation growth that can further change the relationships between runoff and erosion.

MATHEMATICAL MODEL

The Performance Assessment for surface runoff and soil erosion from MDA G require analyses over a duration of 10,000 years or more, but historical records are available for less than 100 years for the Los Alamos area. To provide the record necessary for this performance assessment, a stochastic climate generator is used to provide precipitation and weather values. A daily water balance model of the pit is employed to provide information on seasonal variations of the response of the disposal pit.

The mathematical models for generation of the weather and solution of the water balance were taken from the SPUR (Simulation of Production and Utilization of

Rangelands) Model (Wight and Skiles 1987). The water balance model for SPUR was based on the CREAMS (Chemical, Runoff, and Erosion from Agricultural Management Systems) model (Knisel 1980) with modifications for snow accumulation and melt. Vegetation dynamics were not included in this application of the model. Vegetation was represented by a leaf area index (LAI) curve that remained constant over each year.

The following mathematical descriptions are taken directly from the pertinent chapters in Wight and Skiles (1987).

Climate Generation

The climate generator is known as CLIMGN. The purpose of this component is to provide daily values of precipitation, maximum and minimum air temperatures, and solar radiation (Richardson et al., 1987). The GENPAR code was used to estimate parameters for CLIMGN with historical records from Los Alamos.

The CLIMGN program generates daily values of precipitation (P), maximum temperature (t_{max}), minimum temperature (t_{min}), and solar radiation (r) for an n-year period at a given location. The model is designed to preserve the dependence in time, the internal correlation, and the seasonal characteristics which exist in actual weather data for the location. Precipitation and wind run are generated independently of the other variables. Maximum temperature, minimum temperature, and solar radiation are generated depending on whether the day is wet or dry.

Precipitation

The precipitation-generation component of CLIMGN is a Markov chain-gamma model. A first-order Markov chain is used to generate the occurrence of wet or dry days. When a wet day is generated, the two-parameter gamma distribution is used to generate the precipitation amount.

With the first-order Markov chain model, the probability of rain on a given day is conditioned on the wet or dry status of the previous day. A wet day is defined as a day with 0.01 inch of precipitation or more. Let $P_i(W/W)$ be the probability of a wet day on day i given a wet day on day i-1, and let $P_i(W/D)$ be the probability of a wet day on day i given a dry day on day i-1. Then:

$$P_i(D/W) = 1 - P_i(W/W)$$
$$P_i(D/D) = 1 - P_i(W/D) \qquad (2)$$

where $P_i(D/W)$ and $P_i(D/D)$ are the probabilities of dry day given a wet day on day i-1 and the probability of a dry day given a dry day on day i-1, respectively. The transition probabilities are, therefore, fully defined given $P_i(W/W)$ and $P_i(W/D)$.

The density function of the two-parameter gamma distribution is given by:

$$f(x) = \frac{x^{\alpha-1}e^{-\frac{p}{\beta}}}{\beta^{\alpha}\Gamma(\alpha)}, \qquad p>0 \tag{3}$$

where α and β are distribution parameters and $\Gamma(\alpha)$ is the gamma function of α. The α and β are shape and scale parameters, respectively. For $0 < \alpha < 1$, the distribution has a reverse "J" shape. This shape is appropriate for precipitation amounts since small amounts occur more frequently than larger amounts. The gamma distribution was shown by Richardson (1982a) to better describe precipitation amounts than the simple exponential distribution.

The values of P_i(W/W), P_i(W/D), α, and β vary continuously during the year for most locations. In CLIMGN, each of the four precipitation parameters is held constant for a given month but vary from month to month. The parameters are used with a Markov chain-generation procedure and the gamma-generation procedure described by Haan (1977) to generate daily precipitation values.

Temperature and Solar Radiation

The procedure used in CLIMGN is based on the weakly stationary generating process given by Matalas (1967). The equation is:

$$x_i(j) = Ax_{i-1}(j) + B\varepsilon_i(j) \tag{4}$$

where $x_i(j)$ is a 3 X 1 matrix for day i whose elements are residuals of t_{max}(j=1), t_{min} (j=2), and r(j=3); ε_i is a 3 X 1 matrix of independent random components, and A and B are 3 X 3 matrices whose elements are defined such that the new sequences have the desired serial correlation and cross-correlation coefficients. The A and B matrices are given by:

$$A = M_1 M_0^{-1} \tag{5}$$

$$BB^T = M_0 - M_1 M_0^{-1} M_1^T \tag{6}$$

where the superscripts -1 and T denote the inverse and transpose of the matrix. M_0 and M_1 are defined as:

$$M_0 = \begin{bmatrix} 1.0 & p_0(1,2) & p_0(1,3) \\ p_0(1,2) & 1.0 & p_0(2,3) \\ p_0(1,3) & p_0(2,3) & 1.0 \end{bmatrix} \tag{7}$$

$$M_1 = \begin{bmatrix} p_1(1) & p_1(1,2) & p_1(1,3) \\ p_1(2,1) & p_1(2) & p_1(2,3) \\ p_1(3,1) & p_1(3,2) & p_1(3) \end{bmatrix} \quad (8)$$

where $p_0(j,k)$ is the correlation coefficient between variables j and k on the same day, $p_1(j,k)$ is the correlation coefficient between variables j and k with variable k lagged one day with respect to variable j, and $p_1(j)$ is the lag-one-serial-correlation coefficient for variable j.

The correlation coefficients in Equations 7 and 8 were determined by season from 20 years of temperature and solar radiation data for 31 locations in the United States. The seasonal and regional patterns of the correlation coefficients were described by Richardson (1982b). The seasonal and spatial variation in the correlation coefficients are relatively small. If the small variations are neglected and the average values of the correlation coefficients given by Richardson (1982b) are used, the M_0 and M_1 matrices become:

$$M_0 = \begin{bmatrix} 1 & 0.633 & 0.186 \\ 0.633 & 1 & -0.193 \\ 0.186 & -0.193 & 1 \end{bmatrix} \quad (9)$$

$$M_1 = \begin{bmatrix} 0.621 & 0.445 & 0.087 \\ 0.563 & 0.674 & -0.100 \\ 0.015 & -0.091 & 0.251 \end{bmatrix} \quad (10)$$

(The off-diagonal elements were calculated but not reported by Richardson (1982b).)

Using Equations 5 and 6, the A and B matrices become:

$$A = \begin{bmatrix} 0.567 & 0.086 & -0.002 \\ 0.253 & 0.504 & -0.050 \\ -0.006 & -0.039 & 0.244 \end{bmatrix} \quad (11)$$

$$B = \begin{bmatrix} 0.781 & 0 & 0 \\ 0.328 & 0.637 & 0 \\ 0.238 & -0.341 & 0.873 \end{bmatrix} \quad (12)$$

The A and B matrices given in Equations 11 and 12 are used with Equation 4 in CLIMGN to generate new sequences of the residuals of t_{max}, t_{min}, and r, which are

serially correlated and cross correlated with the correlations being constant at all locations.

The final daily generated values of t_{max}, t_{min}, and r are determined by multiplying the residual elements generated with Equation 4 by a seasonal standard deviation and adding a seasonal mean using the equation:

$$t_i(j) = x_i(j)s_i(j)+m_i(j) \tag{13}$$

where $t_i(j)$ is the daily value of $t_{max}(j=1)$, $t_{min}(j=2)$, and $r(j=3)$; $s_i(j)$ is the standard deviation; and $m_i(j)$ is the mean for day i. The values of $m_i(j)$ and $s_i(j)$ are conditioned on the wet or dry status as determined from the precipitation component of the model. By expressing Equation 13 in terms of the coefficient of variation (c=s/m) rather than the standard deviation, the equation becomes:

$$t_i(j) = m_i(j)[x_i(j)c_i(j)+1] \tag{14}$$

The seasonal change in the means and coefficients of variation may be described by:

$$u_i = \bar{u}+C\cos\left(360\frac{i-T}{365}\right) \qquad i=1,2,...,365 \tag{15}$$

where u_i is the value of $m_i(j)$ or $c_i(j)$ on day i, $\bar{u}$ is the mean of u_i, C is the amplitude of the harmonic, and T is the position of the harmonic in days. Value of u, C, and T must be determined for the mean and coefficient of variation of each weather variable (t_{max}, t_{min}, r) and for the wet or dry condition. There were no detectable differences in the means and coefficients of variation for t_{min} on wet or dry days.

Some of the parameters in Equation 15 demonstrate location dependence, and other parameters do not change significantly with location. The values of T for all the descriptors of temperature (means and coefficients of variation of t_{max} and t_{min}) are near 200 days for all locations. Similarly, the T values for r are about 172 days (summer solstice) for all locations. Therefore, in CLIMGN, all the T values for temperature are assumed to be 200 days and all the T values for solar radiation are assumed to be 172 days.

The $\bar{u}$ and C values for t_{max} vary with location. The amplitude (C) of the mean of t_{max} for a given location was not significantly different on wet or dry days. The C's for the coefficient of variation of t_{max} are negative because t_{max} is less variable during the summer when the mean t_{max} is greatest. The values of $\bar{u}$ and C for the coefficient of variation of t_{max} are the same for either wet or dry days. The $\bar{u}$ values for the mean of t_{max} on wet days were significantly less than for dry days. The other parameters for t_{max} on wet days were not required since they were not significantly different from the

parameters of t_{max} on dry days. The values of $\bar{u}$ and C for the means and coefficients of variation of t_{min} all have a strong regional pattern.

Similar to t_{max}, C for the mean of r was not significantly different on wet and dry days. The values of u and C for the coefficient of variation of r showed no relationship to station location (Richardson et al. 1987). In CLIMGN, the parameter values are assumed to be constant at the average values.

The following notations will be used for the means ($\bar{u}$) and amplitudes (C) of Equation 15 for t_{max}, t_{min}, and r:

TXMD - mean of tmax (dry), °F,
ATX - amplitude of tmax (wet or dry), °F,
CVTX - mean coefficient of variation of tmax (wet or dry),
ACVTX - amplitude of coefficient of variation of tmax (wet or dry),
TXMW - mean of tmax (wet), °F,
TN - mean of tmin (wet or dry), °F,
ATN - amplitude of tmin (wet or dry), °F,
CVTN - mean of coefficient of variation of tmin (wet or dry),
ACVTN - amplitude of coefficient of variation of tmin (wet or dry),
RMD - mean of r (dry), langley(ly),
AR - amplitude of r (wet or dry), ly,
CVRD - mean of coefficient of variation of r (dry), (assumed to be 0.24 for all locations),
ACVRD - amplitude of coefficient of variation of r (dry), (assumed to be -0.08 for all locations),
RMW - mean of r (wet), ly,
CVRW - mean of coefficient of variation of r (wet), (assumed to be 0.48 for all locations),
ACVRW - amplitude of coefficient of variation of r (wet), (assumed to be -0.13 for all locations).

The GENPAR Program

If users need to generate weather data for a location outside the 48 United States or if they need to develop generation parameters from actual data from a specific location, the GENPAR program may be used. The GENPAR program reads daily values of P, t_{max}, t_{min}, and r and writes the generation parameters which are required by CLIMGN. The number of years of weather data required to develop parameters which are representative of a particular location varies with the climate. In general, at least 20 years of precipitation data and 10 years of temperature and radiation data are required. Longer records of precipitation may be required for arid locations. GENPAR was used with Los Alamos and MDA G weather data to estimate the parameters for CLIMGN.

Solar Radiation Correction for Sloping Terrain

A correction factor for adjusting the radiation values generated by the climate model for a horizontal surface to the actual slope and aspect conditions at the site being simulated is included. The procedure uses the method outlined by Lee (1963) to calculate the potential insolation on both a horizontal and an inclined surface.

Water Balance Model

The water balance component is described by Renard et al. (1987). A snow accumulation and melt component also described here can be found in Cooley et al. (1987).

Soil-Layer Water Storage

The soil profile is divided into layers (user-specified number of layers (up to eight) and layer thickness). Water balance calculations are done on a daily basis using runoff, evapotranspiration, and percolation, as described in Equation 1. Total storage, field capacity, and initial water storage in the various layers are expressed in terms of plant available water and are computed from input parameters as follows:

$$UL_i = (SMO_i - SM15_i)THK_i \quad (16)$$

$$FC_i = (SM3_i - SM15_i)THK_i \quad (17)$$

$$SWO_i = FC_i \bullet STF \quad (18)$$

where:

UL_i = upper limit of water storage in layer i (in),
FC_i = field capacity in layer i (in),
SWO_i = initial soil water in layer i (in),
SMOi = soil porosity for layer i (in/in),
$SM3_i$ = 1/3-bar water content for layer i (in/in),
$SM15_i$ = 15-bar water content for layer i (in/in),
THK_i = soil layer thickness for layer i (in), and
STF = initial soil water content as a fraction of field capacity for the entire soil profile.

Runoff

The traditional three antecedent moisture levels (1 - dry, 2 - normal, 3 - wet), as used by the Soil Conservation Service (SCS), have been modified in the model by allowing soil moisture to be updated daily and by computing daily curve numbers based on soil-water storage, rather than using the three curve numbers associated with their moisture classes. Thus, each day has a curve number (Williams and LaSeur 1976), and the soil moisture changes between runoff events with estimates of evapotranspiration and percolation using routines very similar to those used in CREAMS (Knisel 1980). Using the curve number method, surface runoff or Q in Equation 1 is estimated on a daily basis from:

$$Q = \frac{(P - I_a)^2}{P + s - I_a} = \frac{(P - 0.2s)^2}{P - 0.8s} \tag{19}$$

where:

Q	=	daily runoff (in),
P	=	daily rainfall (in),
s	=	a retention parameter (in), and
I_a	=	0.2s = initial abstraction.

The maximum value, s_{mx}, for the retention parameter, s, is computed with the following SCS curve number relationship (USDA 1972):

$$s_{mx} = \frac{1000}{CN1} - 10 \tag{20}$$

where CN1 is the dry-antecedent-moisture-condition curve number. If handbook curve numbers are available for the normal moisture condition, CN2, the following polynomial may be used to estimate CN1:

$$CN1 = -16.91 + 1.348CN2 - 0.01379CN2^2 + 0.0001177CN2^3 \tag{21}$$

The soil retention parameter scales from zero to s_{mx} and is computed daily as a weighted average of the unused storage in the various soil layers. The retention parameter is:

$$s = s_{mx} \sum_{i=1}^{n} \left(W_i \frac{UL_i - SW_i}{UL_i} \right) \tag{22}$$

where:

n	=	number of soil layers,

SW_i = current water storage in layer i (updated daily) (in), and
W_i = weighting factor.

The weighting factors decrease exponentially to give greater dependence of s on the upper soil layers, so:

$$W_i = a e^{-4.16 d_i} \tag{23}$$

where:
d_i = (depth to bottom of layer i)/(depth to bottom of last layer), and
a = constant adjusted so that $\sum_{i=1}^{n} W_i = 1$.

Percolation

The percolation component of SPUR uses a storage routing model combined with a crack-flow model to predict flow through the soil profile. Crack-flow was not implemented for these simulations.

In the following, PL_i is percolation flow out of the bottom layer i from the storage routing model. The variable PL_o is equal to precipitation minus runoff, and it is the amount of water that enters the first soil layer.

Flow through a soil layer may be restricted by a lower layer which is saturated or nearly saturated. The variable PL_i may exceed the projected available storage in the next layer (UL_{i+1} - SW_{i+1} + UW_{i+1}), in which case, PL_i is set to this projected value (see Equation 39 for definition of UW_{i+1}). There is no "succeeding" layer to the bottom layer, and the value for R in Equation 1 is PL_i for the bottom layer.

Storage Routing

The storage routing model uses an exponential function with the percolation computed by subtracting the soil water in excess of field capacity at the end of the day from that at the beginning of the day, or:

$$PL_i = \begin{cases} (SW_i - FC_i)\left(1 - e^{-\frac{\Delta t}{T_i}}\right) & SW_i > FC_i \\ 0 & SW_i \le FC_i \end{cases} \tag{24}$$

where:

PL_i = amount of percolate (in),
SW_i = the soil water content at the beginning of the day for layer i (in)
Δt = time interval (24 h),
T_i = travel time through a particular layer (h),
FC_i = the field capacity water content for layer i, (in), and
i = soil layer number increasing with depth.

The travel time through each soil layer is computed with the linear storage equation:

$$T_i = \frac{SW_i - FC_i}{H_i} \tag{25}$$

where: H_i = the hydraulic conductivity of layer i (in/h).

Hydraulic conductivity is varied from the specified saturated conductivity value by:

$$H_i = SC_i\left(\frac{SW_i}{UL_i}\right)^{\beta_i} \tag{26}$$

where:

SC_i = saturated conductivity for layer i (in/hr), and
β_i = parameter that causes $H_i = 0.0022\ SC_i$ when $SW_i = FC_i$.

The equation for estimating β_i is:

$$\beta_i = \frac{-2.655}{\log\left(\frac{FC_i}{UL_i}\right)} \tag{27}$$

where the constant (-2.655) assures that $H_i = 0.0022\ SC_i$ at field capacity.

Evapotranspiration

The evapotranspiration (ET) component in SPUR is the same as that used in CREAMS and is based on work by Ritchie (1972). Potential evaporation is computed with the equation:

$$E_o = \frac{0.0504\,H_o\Delta}{\gamma + \Delta} \tag{28}$$

where:
E_o = potential evaporation (in),
Δ = slope of the saturation-vapor-pressure curve at the mean air temperature,
H_o = net solar radiation (ly), and
γ = a psychrometric constant.

Δ is computed with the equation:

$$\Delta = \frac{5304}{T_k^2} e^{\left(21.255 - \frac{5304}{T_k}\right)} \quad (29)$$

where: T_k = daily temperature (degrees Kelvin).

The variable H_o is calculated with the equation:

$$H_o = \frac{(1-\lambda)r}{58.3} \quad (30)$$

where:
r = daily solar radiation (ly) and
λ = albedo.

Soil evaporation

The model computes soil evaporation and plant transpiration separately. Potential soil evaporation is computed with the equation:

$$E_{so} = \min\begin{cases} E_o e^{-0.4LAI} \\ E_o GR \end{cases} \quad (31)$$

where:
E_{so} = potential evaporation at the soil surface (in),
LAI = Leaf area index defined as the area of plant leaves relative to the soil surface (in^2/in^2), and
GR = mulch (residue) cover factor. (A value of 0.5 is suggested for most range plant communities, and 1.0 for bare soil.)

Actual soil evaporation (E_s) is computed in two stages based on the soil moisture status in the upper soil profile. In stage 1, soil evaporation is limited only by the energy available at the surface, and thus, is equal to the potential (Eq. 31). When the accumulated soil evaporation exceeds the first-stage upper limit, the stage-2

evaporation begins (the reader is referred to Ritchie (1972) for additional explanation of the procedure). The first-stage upper limit is estimated from:

$$U = 1.38(\alpha - 0.118)^{0.42} \tag{32}$$

where:
U = stage-1 upper limit (in) and
α = soil evaporation parameter (CONA) dependent on soil-water transmission characteristics (ranges from 0.13 to 0.22 in/day$^{1/2}$).

Ritchie (1972) suggests using α=0.14 for clay soils, 0.18 for loamy soils, and 0.13 for sandy soils. Similar values were obtained for data from Jackson et al. (1976). A wider distribution of values for most soil textural classes is given by Lane and Stone (1983).

Stage-2 soil evaporation is predicted by:

$$E_s = \alpha\left[t^{\frac{1}{2}} - (t-1)^{\frac{1}{2}}\right] \tag{33}$$

where:
E_s = soil evaporation for day t (in) and
t = days since stage-2 evaporation began.

Plant transpiration

Potential transpiration (E_{po}) from plants is computed with the equations:

$$E_{po} = \frac{E_o LAI}{3} \qquad 0 \le LAI \le 3 \tag{34}$$

$$E_{po} = E_o - E_s \qquad LAI > 3 \tag{35}$$

(If $E_{po} + E_s > E_o$, E_s is reduced so $E_{po} + E_s = E_o$.) Because the LAI is generally less than three in rangeland plant communities that SPUR is intended to consider, Equation 34 will be used most of the time. If soil water is limited, plant transpiration is reduced with the equation:

$$E_p = \frac{E_{po} SW}{0.25FC} \qquad SW \le 0.25FC \tag{36}$$

where:
E_p = plant transpiration reduced by limited soil moisture (in) and
SW = current soil water in the root zone (in).

(If SW > 0.25 (FC), $E_p - E_{po}$, and if $E_p + E_s$ exceeds available water, E_s is reduced so $E_p + E_s$ = available water.)

Evapotranspiration (ET), then, is the sum of plant transpiration (Eq. 34, 35 or 36) plus soil evaporation (Eq. 32 or 33), and cannot exceed available soil water.

Distribution of ET in the soil profile

Soil-water evaporation is removed uniformly from the soil profile down to a maximum depth (ESD). The variable ESD is set in the SPUR code. If the soil profile does not contain sufficient water to meet soil-water evaporation demand, the actual amount of evaporation is reduced accordingly.

Transpiration is initially distributed through the soil layers by the following equation:

$$v = v_0 e^{-v_1 D} \tag{37}$$

where:

v = water-use rate by crop at depth D (in/day),
v_o = water-use rate at the surface (in/day),
V_1 = 3.065, and
D = soil depth/depth to bottom of deepest soil layer with roots.

The total water use within any depth can be computed by integrating Equation 37. The value of v_o is determined for the root depth each day, and the water use in each soil layer is computed with the equations:

$$v_o = \frac{v_1 ET}{1 - e^{-v_1}} \tag{38}$$

$$UW_i = \frac{v_o}{v_1}\left(e^{-v_1 D_{i-1}} - e^{-v_1 D_i}\right) \tag{39}$$

where:

UW_i = water use in layer i (n), and
D_{i-1} and D_i = the fractional depths at the top and bottom layer i.

When calculating actual uptake, transpiration demand for a layer that cannot be satisfied by the available water in that layer is added to the demand of the next layer. This process is continued until the transpiration demand is satisfied or the bottom of the root zone is reached.

The UW_I vector contains the initial estimates of ET which are to be subtracted from the various soil layers. If a layer has insufficient water, the excess ET is taken out of the first layer containing available water and having roots present.)

Soil Erosion

Soil erosion is calculated using the modified Universal Soil Loss Equation (Williams 1975). The equation is

$$Y = \eta\left(Q * Q_p\right)^{0.56} KCPLS \qquad (40)$$

where:

Y	=	sediment yield (tons/acre),
η	=	coefficient = 95,
Q	=	runoff volume (in),
Q_p	=	peak flow rate (ft^3/s),
K	=	Universal Soil Loss Equation (USLE) soil erodibility factor,
C	=	USLE cover management factor,
P	=	USLE erosion control practice factor, and
LS	=	USLE slope length and steepness factor.

Snow Accumulation and Melt

The model used for snow accumulation and melt processes is HYDRO-17, developed by Anderson (1973) of the National Weather Service (NWS).

HYDRO-17 incorporates physical processes affecting snow accumulation and melt. Air temperature is used to index energy exchange across the snow-air interface. This is not the same as the degree-day method, which uses air temperature as an index to snowpack outflow. The degree-day method does not explicitly account for freezing of the melt water due to a heat deficit and the retention and transmission of liquid water, both of which cause snowpack outflow to differ from snowmelt.

Accumulation process

The accumulation of snow in the model is simply based on the air temperature and the temperature selected to differentiate rain from snow (PXTEMP). Precipitation is considered to be snow if the air temperature is less than or equal to PXTEMP, and rain if the air temperature is greater than PXTEMP. The amount of new snow is added to the existing snowpack to establish a new total snowpack.

Melt processes

The snowmelt processes are divided into two categories: snowmelt during rain-on-snow and snowmelt during nonrain periods. Snowmelt during rain-on-snow periods is separated from melt during nonrain periods because (1) of the difference in magnitude of the various energy transfer processes during rain-on-snow periods, and (2) the seasonal variation in melt rates is generally different for the two processes.

Rain-on-snow

During rain-on-snow, melt is assumed to occur at the snow surface. Following the development of the model relationships presented by Anderson (1973), the energy balance of a snow cover can be expressed as:

$$\Delta Q = Q_n + Q_m + Q_e + Q_h + Q_g \qquad (41)$$

where:

ΔQ = change in the heat storage of the snow cover,
Q_n = net radiation transfer,
Q_m = heat transfer by mass changes (advected heat),
Q_e = latent heat transfer,
Q_h = sensible heat transfer, and
Q_g = heat transfer across the snow-soil interface.

The units of each term in Equation 41 are energy per unit area.

Upon expansion of each term in Equation 41, and elimination of variables made possible by the assumptions listed below, the amount of snowmelt M (mm) during a time period Δt (h) can be determined as follows:

$$M = \Delta t\left[0.612\times10^{-9}\left(T_a+273\right)^4-3.39\right]+0.0125\,P_x T_a + 8.5\,UADJ\left[\left(0.9\,e_{sat}-6.11\right)+0.00057\,P_a T_a\right] \qquad (42)$$

where:

T_a = temperature of the air (°C),
P_x = water equivalent of precipitation (mm),
P_a = atmospheric pressure (mb),
e_{sat} = saturation vapor pressure at the air temperature (mb), and
UADJ = average wind function during rain-on-snow periods (mm • mb^{-1} Δt h^{-1}).

The assumptions pertaining to conditions during rain-on-snow events are as follows:

1. The turbulent transfer coefficients for heat and water vapor are equal.

2. The temperature of the snow cover outflow is 0 °C.
3. The heat content of the transferred vapor is negligible; only heat transferred by precipitation is considered.
4. The isothermal snow cover is melting and the snow surface temperature is 0 °C.
5. Heat transfer across the snow-soil interface is negligible compared with energy exchange at the snow surface.
6. The change in heat storage of the snow surface becomes equal to the amount of melt.
7. Incoming longwave radiation is negligible because overcast conditions prevail.
8. Incoming longwave radiation is equal to blackbody radiation at the temperature of the bottom of the cloud cover, which should be close to the air temperature.
9. The relative humidity is quite high (90 percent is used).

Under the conditions described by these assumptions, the wet-bulb temperature is essentially the same as the air temperature. The saturation vapor pressure can be computed as a function of air temperature by the relationship:

$$\dot{e}_{sat} = 2.749 \times 10^{8}\, e^{\left[\frac{-4278.6}{T_a + 242.8}\right]} \tag{43}$$

The atmospheric pressure, P_a, is computed for the elevation of the site or area using a "standard atmosphere" altitude-pressure relationship which can be approximated by the expression:

$$P_a = 1012.4 - 11.34\,E_t + 0.00745\,E_t^{2.4} \tag{44}$$

where E_t = elevation (hundreds of meters).

The wind-function parameter, UADJ, is determined during the calibration process. In the model, the amount of rain must exceed 6 mm during a 24-hour period before Equation 42 is used; therefore, humid overcast conditions are more likely to have occurred.

Ablation (Nonrain Periods)

Because such a wide variety of meteorological conditions can occur during nonrain periods, the energy balance equations are not used as a basis for estimating snowmelt from air temperature. Rather, an empirical air-temperature-based relationship is used in which snowmelt is determined by:

$$M = M_f(T_a - MBASE) \tag{45}$$

where:

M_f = melt factor,
MBASE = base temperature (°C) below which no melt is produced, and
T_a = air temperature (°C).

The melt factor exhibits a seasonal variation due partly to the variation in incoming solar radiation, and partly to a decrease in the albedo of the snow cover with time since the last snowstorm, Seasonal variations in other meteorological factors like vapor pressure, wind, and cloud cover, also influence the melt factor. A sinusoidal relationship between melt factor and season was developed within the model to account for this variation. This relationship is adequate for use throughout the 48 contiguous United States.

Groundmelt

In some watersheds, a small amount of melt takes place continuously at the bottom of the snowpack. The melt is small on a daily basis, but it can amount to a significant quantity of water when accumulated over an entire snow season. Groundmelt adds to soil moisture storage and helps sustain baseflow throughout the winter. It is added to the snow cover outflow and to rain which falls on bare ground to obtain total rain plus melt.

Model Parameters for Snow Accumulation and Melt

In addition to the data requirements of temperature, and site elevation, values must be set for six major and six minor parameters to use the model. The six major parameters are those which generally have the greatest effect on the simulation results and, therefore, require the most care in determining the proper value. These parameters with their expected range in parentheses are:

1. SCF -- (0.8 - 1.4). A snow correction factor which adjusts precipitation for gage-catch errors during periods of snowfall and implicitly accounts for net vapor transfer and interception losses. This parameter depends mainly on the wind speed at the gage site and whether the gage is shielded.
2. MFMAX -- (2.0 - 8.0) (mm/°C - 24 h). Maximum-melt factor during nonrain periods. This factor is affected by many climatic and physiographic variables such as radiation intensity, wind, forest cover, and aspect.
3. MFMIN -- (0.4 - 3.6) (mm/°C - 24 h). Minimum-melt factor during nonrain periods. The same climatic and physiographic variables that affect MFMAX also effect MFMIN in essentially the same way.
4. UADJ -- (0.0 - 0.6) (mm/mb). The average wind function during rain-on-snow periods, which is affected most by density and height of vegetation, and terrain.

5. SI -- (200 - 600) (mm). The mean, areal water equivalent above which there is always 100 percent areal snow cover. This value is affected by the snowfall characteristics of the area. If the snow cover is uniform and melts at a uniform rate, the area will remain at 100 percent cover until just before the snow disappears. In contrast, especially where drifting occurs, the snow cover in some areas is so variable that bare ground appears as soon as melt begins.
6. ADPT -- Areal Depletion Curve (described more fully later). A curve which defines the areal extent of the snow cover as a function of how much of the original snow cover remains. It also implicitly accounts for the reduction in the melt rate that occurs with a decrease in the areal extent of the snow cover and is closely related to the SI parameter.

The six minor parameters can normally be determined in advance, based on a knowledge of the typical climatic and snow cover conditions for the area. These parameters and their normal range of values in parentheses are:

1. TIPM -- (0.1 - 0.5). A factor that determines how much weight is placed on the air temperature for each prior period. A small value corresponds to deep snowpacks and longer periods, while a larger value corresponds to shallow snowpacks and short periods of only a few days.
2. NMF -- (0.0 - 2.0)(mm/°C/24 h). The maximum negative melt factor. This factor is assumed to have the same seasonal variability as the surface melt factor. It is affected mostly by snow density, though climate and physiographic variables also affect heat exchange during nonmelt periods.
3. MBASE -- (0.0 - 2.0)(°C). Base temperature (normally 0 °C) for snowmelt computations during nonrain periods.
4. PXTEMP -- (0.0 - 5.0) (°C). The temperature which differentiates rain from snow (normally 1 to 2 °C).
5. PMWHC -- (0.01 - 0.05). Percent liquid-water holding capacity expressed as a decimal. Represents the maximum amount of liquid water in the snowpack which can be held against gravity drainage.
6. DAYGM -- (0.0 - 0.5)(mm). Constant rate of melt which occurs at the snow-soil interface whenever the soil is not frozen and snow is present.

The range of values presented are based on information reported by Anderson (1973) and experience in calibrating the model at several sites and climatic regimes. Although upper and lower values are presented, values outside this range can occur. Since the model has been tested over such a wide range of conditions, most of the values should be within the range presented.

PARAMETER ESTIMATION

Springer (1995) performed an initial simulation of MDA G using the same mathematical model. Since that simulation, additional information and data are available to change the estimates of many of the parameters. The following sections provide the estimates for the parameters required by the surface runoff and erosion model that has been presented in the previous section.

Weather Realizations

Daily observations of precipitation at Los Alamos extend back to 1920 with a one-year break during 1944. The Los Alamos precipitation gauge has been moved several times, but Nyhan et al. (1989) found that the location changes have had no effect on annual precipitation. As the Laboratory developed, additional precipitation gauges have been installed at different sites including MDA G and White Rock. The main Los Alamos precipitation gauge was located at TA-59 which is west of MDA G and at a higher elevation, and since 1990 the main Los Alamos gauge has been located at TA-6 which is south of TA-59 In this report, TA-59 will designate the main Los Alamos gauge even though data from TA-6 is included in the analysis.

The longest available record of weather data is from TA-59 or the Los Alamos gauge. The average annual precipitation at TA-59 is 45.7 cm compared to 35.6 cm from MDA G (Bowen 1990). The length of record is relatively short compared to the simulation times involved, but still the TA-59 location was used to estimate the needed parameters for the precipitation realizations. The GENPAR program was used with data from 1951 to 1994 to make the parameter estimates for CLIMGN. For days with missing precipitation, a value of 0.0 was entered. Parameter estimates for TA-59 are given in Table 2. The average annual precipitation using these parameters for a 10000-year simulation was 47.8 cm.

Table 2. Parameters for CLIMGN used to generate precipitation realizations for MDA G simulations.

Month	P(W/W)	P(W/D)	Alpha	Beta
Jan	0.426	0.121	0.759	0.215
Feb	0.389	0.168	0.846	0.146
Mar	0.469	0.166	0.824	0.191
Apr	0.447	0.127	0.732	0.223
May	0.534	0.156	0.797	0.217
Jun	0.477	0.151	0.752	0.254
Jul	0.598	0.347	0.744	0.299
Aug	0.613	0.369	0.788	0.327
Sep	0.518	0.191	0.717	0.294
Oct	0.494	0.120	0.734	0.344
Nov	0.455	0.115	0.796	0.253
Dec	0.420	0.130	0.765	0.236

The Los Alamos precipitation data is adding an additional 10 cm of precipitation on average over that received at MDA G. The advantage of the Los Alamos data is a longer record with better parameter estimates. One approach is to reduce the Los Alamos data by a linear factor so that the average annual precipitation is equal to 35.6 cm. The problem with this approach is the seasonal or monthly dynamics between the sites may be different. Using the White Rock / MDA G precipitation record from 1965 to 1994, a GENPAR estimate of the parameters required for CLIMGN was made. Comparisons between the CLIMGN precipitation parameters from both TA-59 and MDA G for the period of record in which there are values are given in Figures 5-8. The differences between sites appear to be consistent and no crossing in the monthly behavior is obvious between sites. Generally all parameter values for Los Alamos are greater than those from White Rock except the alpha parameter which is consistently larger for White Rock. Richardson et al. (1987) defined the alpha as the shape parameter for the gamma distribution therefore the higher alpha values for White Rock indicate a larger variance or more spread in these data. It was assumed that the consistent differences observed between the parameters in Figures 5-8 permitted the Los Alamos data to be reduced by a constant factor so that average annual precipitation for the 10000-year simulation was 35.6 cm.

Temperature and solar radiation data from TA-54 were used for parameter estimates for the variables in CLIMGN because the nearest weather station is Albuquerque and parameters from Hanson and Richardson (1987) for Albuquerque were not considered adequate. The parameter values used in the simulations are given in Table 3.

Table 3. Temperature and solar radiation parameters for CLIMGN for base case simulation.[1]

Parameter Name	Value
TXMD	62.3
ATX	21.4
CVTX	0.127
ACOTX	-0.074
TXMW	55.51
TN	37.1
ATN	18.6
CVTN	0.203
ACUTN	-0.164
RMD	487.0
AR	196.2
RMW	365.6

[1]Wind run was not used as part of this simulation.

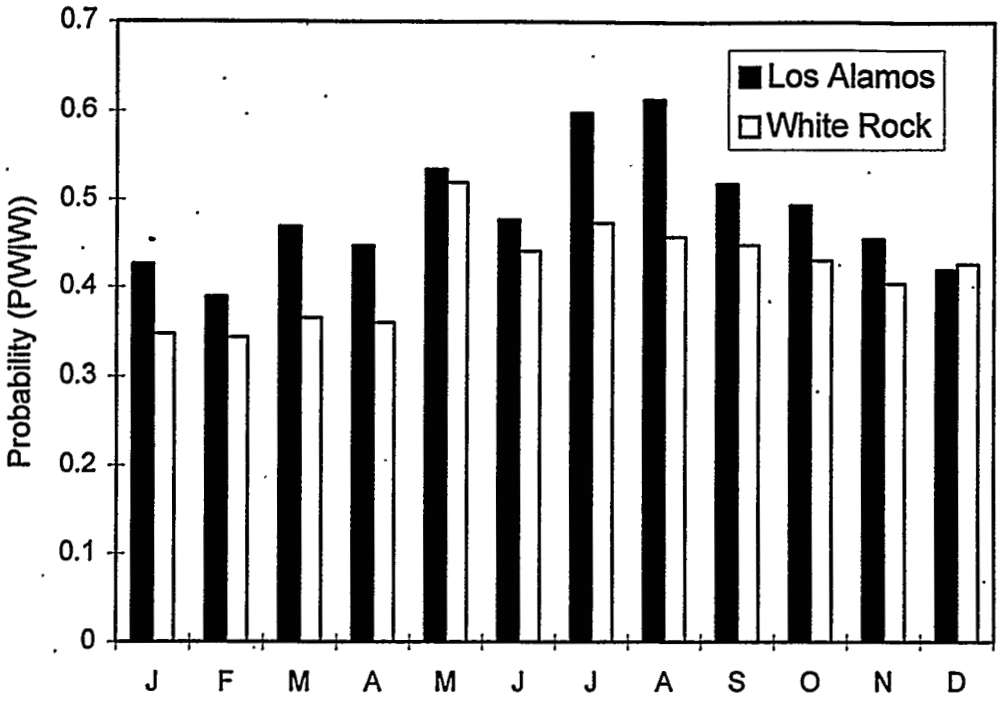

Figure 5. Comparison between Los Alamos and White Rock (MDA G) of probability of a wet day given a wet day.

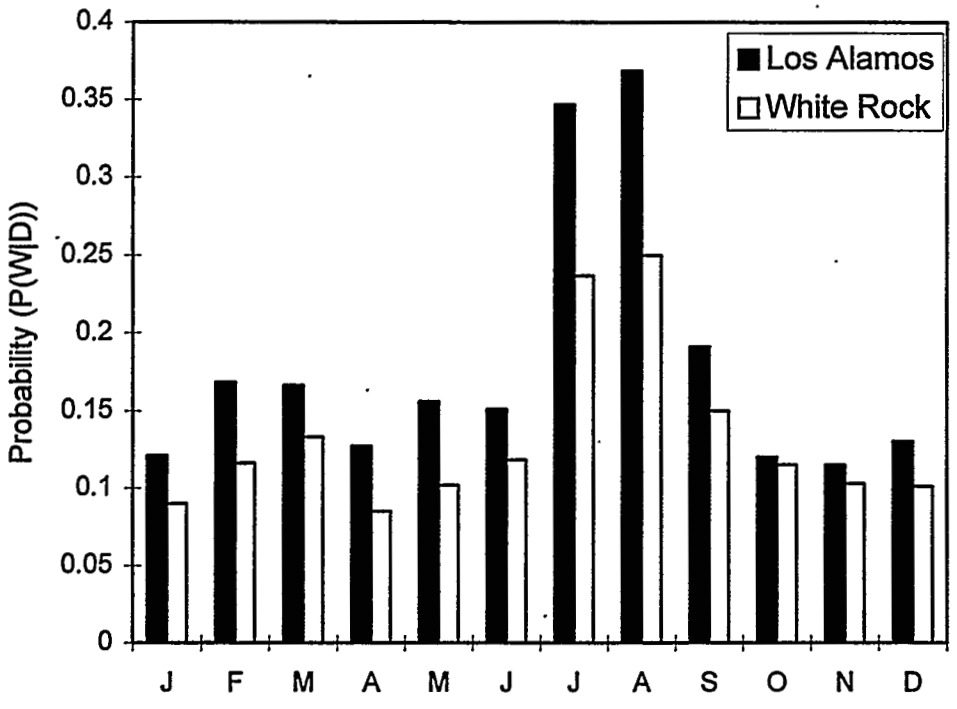

Figure 6. Comparison between Los Alamos and White Rock (MDA G) of the probability of a wet day given a dry day.

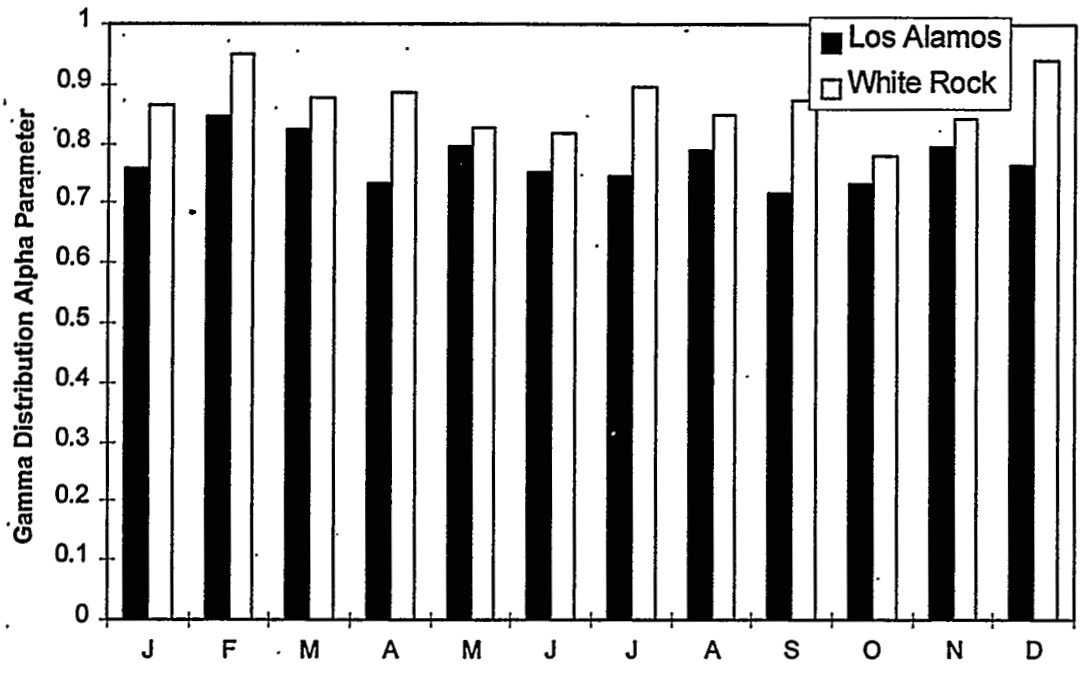

Figure 7. Comparison between TA-59 and TA-54 (MDA G) of the gamma distribution alpha parameter for daily precipitation amount.

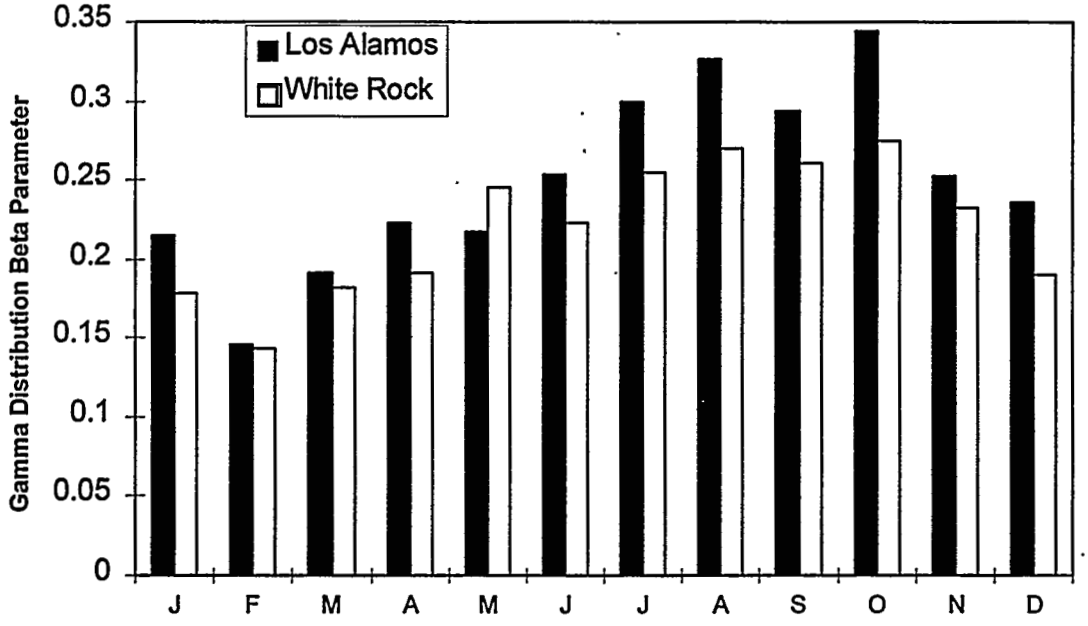

Figure 8. Comparison between TA-59 and TA-54 (MDA G) of the gamma distribution beta parameter for daily precipitation amount.

Soil Properties

The pit for this simulation was given a surface area of 0.41 ha (1 ac) with a length to width ratio of 2:1. The pit was assumed to be sloped along the width dimension for runoff and erosion calculations. The surface slope was 3 percent. The pit with cover was assumed to be 16.25 m (53.3 ft.) deep, but the water balance for the upper 1 m (3 ft.) was simulated for this effort to supply water input for source-term calculations.

A clay loam surface soil was used as most representative of the Hackroy soil series found in this part of Los Alamos (Nyhan et al. 1978). The depth of the topsoil layer was 10 cm (4 in.). The hydrologic properties for the clay loam soil were obtained from Nyhan (1996, pers. comm.) for soil from plots located at TA-51. These data are a better representation than the average values for a clay loam texture class from Springer and Lane (1987) used by Springer (1995). The data from Nyhan (1996, pers. comm.) was in the form of a moisture characteristic and the RETC code from van Genuchten et al. (1991) was used to fit the van Genuchten (1980) function to the data to estimate the 340 cm and 15300 cm volumetric water contents. The parameter estimates from RETC are: saturated water content = 0.493; residual water content = 0.0673; alpha (cm^{-1}) = 0.0115; and N = 1.5031. The values used in the water balance simulations are given in Table 4.

The remaining depth (90 cm) of the pit was filled with crushed Bandelier Tuff which is the common backfill at MDA G. Springer (1995) used the results from van Genuchten et al. (1987) who fit a soil water retention function to data from an instantaneous profile experiment that used crushed Bandelier Tuff in an intermediate-scale facility. The tuff for that intermediate-scale experiment was obtained from the quarry at Los Alamos, and it was most likely from unit 3 of the Bandelier Tuff rather than unit 2 in which most of the pits at MDA G are located. Abeele et al. (1986) characterized the moisture retention on several cores from boreholes at TA-54 including MDA G, but Abeele et al. (1986) did not provide bulk density or porosity data for their samples. Porosity and bulk density estimates for the Bandelier Tuff units characterized by Abeele et al. (1986) were obtained by using the means for the same units from Rogers and Gallaher (1995). The data from Abeele et al. (1986) were analyzed using the RETC code (van Genuchten et al. 1991). The estimated parameters for the van Genuchten (1980) function for the crushed tuff were: saturated water content = 0.479; residual water content = 0.008; alpha (cm^{-1}) = 0.007; and N = 2.004. The parameter estimates for the water balance model are given in Table 4. The estimated saturated hydraulic conductivity for the crushed Bandelier Tuff is the same as that from Springer (1995) because there was no additional data on this parameter.

Table 4. Soil and crushed tuff properties used for MDA G simulation.

	Hackroy Clay Loam	Crushed Tuff
Porosity	0.493	0.479
1/3-bar volumetric water content	0.273	0.1982
15-bar volumetric water content	0.099	0.0122
Saturated hydraulic conductivity (cm/hr)	0.899	1.270

The 1-m soil profile was divided into eight layers. The thickness of layers 1 through 6 was 5 cm (2 in.), layer 7 was 15.2 cm (6 in.), and layer 8 was 55.8 cm (22 in.).

The value for the soil evaporation parameter in Equation 32, CONA, is 3.8 $mm/day^{1/2}$ which is the suggested average value for the clay loam texture class.

Data were available for runoff from MDA G for two subwatersheds that were monitored by the Stormwater Runoff Program operated by ESH-18 at Los Alamos. Data for these subwatersheds denoted G-1 and G-3 are given in Table 5. It can be seen from Table 5 that there were a limited number of events recorded during the 1995 water year. Also, the last column of Table 5 is the estimated curve number parameter using relationships from Springer et al. (1980) to estimate the CN value for a given precipitation - runoff data pair. The lowest CN value observed was 72.5. What is not shown in Table 5 is the number of events where precipitation occurred with no runoff. These data reduced the CN1 to 70 for these simulations of MDA G. This is consistent with the CN2 from Lane (1984) for the Los Alamos CREAMS simulations. Using Equation 21 a CN2 of 85 has an estimated CN1 of 70.2.

Table 5. Runoff data from MDA G watersheds collected by Stormwater Runoff Program at Los Alamos.

Watershed	Date	Precipitation	Runoff	Estimated CN
		(mm)	(mm)	
G-1	5/29/95	28.19	0.76	72.5
G-1	8/13/95	14.48	0.18	82.0
G-1	8/29/95	17.02	2.73	89.0
G-1	9/7/95	26.42	2.39	79.9
G-3	8/29/95	17.02	0.38	80.8
G-3	9/7/95	26.42	0.97	75.1
G-3	9/8/95	26.42	1.79	78.1

The LAI distribution was taken from Lane (1984) for his Los Alamos simulation with CREAMS. These values and their Julian date are given in Table 6. Linear interpolation is used between Julian days to determine LAI values between the days listed in Table 6. Rooting depth was assumed to be 0.45 m (1.5 ft.). This parameter was varied for sensitivity analyses because the depth in the soil profile from which water is extracted is

determined by the rooting depth. By removing water deeper from the profile, percolation will be affected.

Table 6. Leaf area index distribution used for MDA G simulation.

Julian Day	Leaf Area Index
1	0.0
91	0.02
121	0.05
152	0.20
182	1.00
213	1.00
244	0.80
274	0.20
305	0.01
366	0.0

For these simulations, rapid or crack flow and return flow were set to zero. The disturbed nature of the pit and packing of crushed materials reduce the opportunity for rapid flow by destroying the structure of the soil and tuff. The design of the base case cover does not include permeability barriers that can create significant lateral flow.

Soil Erosion Parameters

Tables, charts, and data from Nyhan and Lane (1986b) for Los Alamos were used to estimate the parameters for MUSLE (Equation 51). Slope length was 30 m (98.4 ft.) and the slope was 3 percent giving the LS factor a value of 0.28. The K factor was the average value obtained from the 1983 simulations of Nyhan and Lane (1986b) of 0.069 Mg ha h/MJ ha mm (0.52 ton·acre hour/100 acre·ft-ton·inch). The C or cover factor of 0.03 was taken from the 1983 simulator run of Nyhan and Lane (1986b) for their trench cap plots with a gravel and wheatgrass cover.

SIMULATION RESULTS

The surface runoff, soil erosion, and percolation through the 1-m cover at MDA G were predicted using a Monte Carlo approach. A total of 100 realizations that were 10000 years long were generated in this Monte Carlo procedure giving a total of 1000000 annual observations for the response variables. The 10000-year period was selected for sensitivity and uncertainty analyses purposes according to guidance from DOE. The percolation estimates are used by the subsurface transport pathway to predict radionuclide source term behavior and transport from the pits.

The statistics for the annual precipitation from the weather generator were:

mean = 35.56 cm (14.0 in),
standard deviation = 5.97 cm (2.35 in.),
maximum annual = 71.02 cm (27.96 in.), and
minimum annual = 12.29 cm (4.84 in.).

Nyhan et al. (1989) estimated the 100-year annual precipitation event for the Los Alamos gauge to be 83.57 cm (32.9 in.). The Nyhan et al. (1989) estimate compares well with the maximum generated by the stochastic weather generator.

Statistic for the three response variables are given in Table 7. The percolation value is for the bottom of a 1-m profile.

Table 7. Statistics for annual values of percolation, runoff, and soil erosion for 100 Monte Carlo simulations each with a realization length of 10000 years (total of 1000000 observations) for MDA G at Los Alamos.

Variable	Mean	Standard Deviation	Maximum	Minimum
Percolation (mm)	0.99	5.17	129.33	0.0
Runoff (mm)	0.78	1.65	67.49	0.0
Soil erosion (t/ac•yr)	0.002	0.005	0.23	0.0

The large standard deviations relative to the means for each variable are indicative of highly dispersed distributions, and the large maximum values suggest a skewed distribution. These results are consistent with those of Springer (1995) in terms of the relationship between the statistics. The magnitude of the values are lower than those from Springer (1995) because of the reduced mean annual precipitation and changes in the CN1 and soil water properties of the cover profile.

Springer (1995) found that over 80 percent of the annual percolation values were zero. The same results hold for this data set. Some confidence in the simulation results can be gained through the annual distribution of percolation. Nyhan et al. (1990) reported that percolation through a conventional cover was greatest in the late winter and early spring when snowmelt occurred and evapotranspiration was low because the vegetation was not active. Figure 9 is a plot of the monthly mean percolation from the Monte Carlo simulation. The sum of the February and March percolation values is approximately 68 percent of the annual average of 0.99 mm.

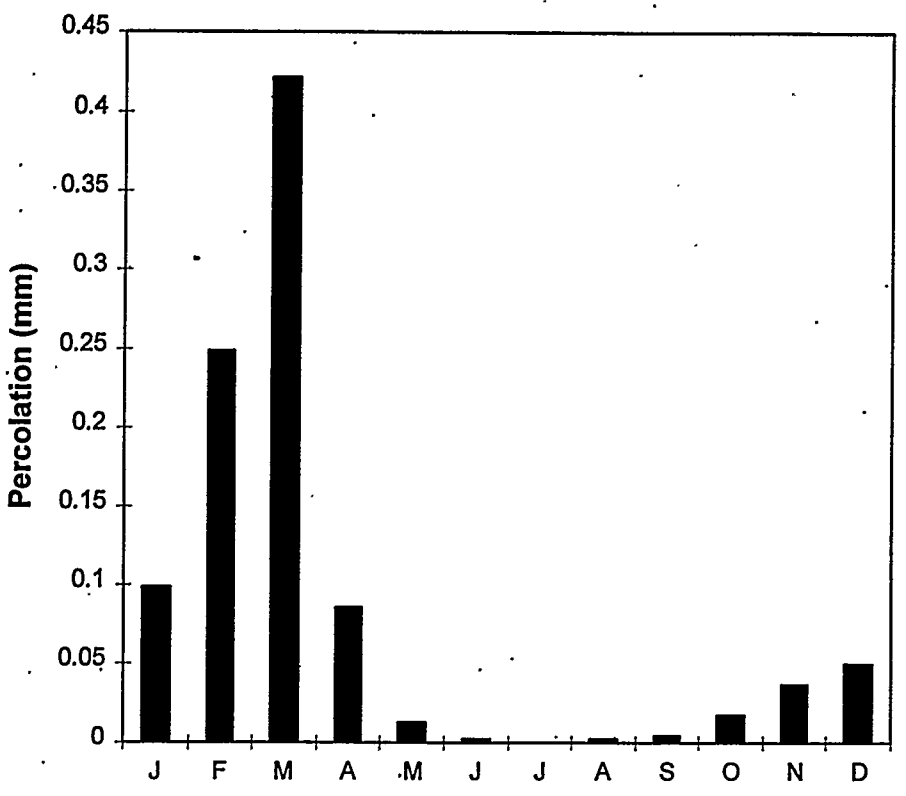

Figure 9. Average monthly percolation for MDA G from 100 Monte Carlo simulations with a realization length of 10000 years.

The average surface runoff in Table 7 is low compared to the available runoff data from MDA G in Table 5. The limited amount of available data cannot be considered representative of long-term response. These data were used to estimate the minimum CN, but this is not an average. To estimate the average, it is estimated that 30 years of data are required. Another issue for runoff generation is the use of a daily precipitation and the CN method. In the Los Alamos area, high intensity rainfall events generate runoff and soil erosion, and the daily precipitation moderates the rainfall intensity effect because rainfall duration is constant for precipitation event. An alternative approach is to use the daily simulation model for the interstorm period and an event based model such as KINEROS (Woolhiser et al., 1990) for the high intensity rainfall events. One complication is that the event based model will require more data on spatial distribution of infiltration and surface hydraulic properties.

The soil erosion in Table 7 is well below the EPA recommended rate of 4.48 mT/ha•yr (2 t/ac•yr). This low erosion rate is directly related to the low runoff. Taking the maximum rate from Table 7, the 1-m surface cover will be erode so that waste is expose in 10000 years (≈ 0.0005 cm/yr). This calculation assume a spatially uniform rate of soil removal and a bulk density of the material of 1.337 g/cm^3 (Abeele 1984).

This result is also dependent on the maintenance of the vegetation and gravel mulch cover that has been shown to be effective at erosion control (Nyhan et al. 1984). The persistence of the gravel mulch and grass cover is unknown.

UNCERTAINTY AND SENSITIVITY

The range of the variables in Table 7 reveals considerable uncertainty. The range of percolation is three orders of magnitude which is similar to the range reported by Springer (1995). Percolation is important because it is used by the subsurface pathway analysis to predict subsurface radionuclide migration. More site specific data from MDA G were used for parameter estimates of the daily water balance model in this simulation than used by Springer (1995), but the uncertainty has not been substantially reduced. Much of the uncertainty in the percolation and runoff results is due to the weather input term, and with realistic parameter estimates in the water balance model little reduction in uncertainty is possible.

Springer (1995) examined the sensitivity of CN1, LAI, rooting depth (RD), and initial soil water content and found that the CN1 and RD parameters were significant relative to surface runoff and percolation response. These results were consistent with those from Lane and Ferreira (1980) for the CREAMS model. Additional data from MDA G has given a better estimate of the CN1 so this parameter has been fixed. RD was increased to a depth of 1 m which decreased the average annual percolation to 0.003 mm and the maximum annual percolation to 69 mm. This parameter remains sensitive, but further refinement is difficult without more controlled experimentation. Also, the data from the chloride profile studies by Newman (1996) supports higher flux rates in this upper zone. LAI was reduced in half with the same temporal distribution and the mean percolation rate was doubled (2.08 mm vs. 0.99 mm). The change of magnitude in LAI had a limited effect on mean surface runoff (0.78 mm vs. 0.99 for the 0.5*LAI case). LAI can be measured reducing uncertainty associated with this parameter. Measurement of LAI will also provide some data on its seasonal distribution which has not been addressed in these simulations.

Long-term dynamics of the vegetation and soil properties remains unknown in these simulations. These effects can be very important to the integrity of surface covers (Suter et al., 1993).

SUMMARY AND RECOMMENDATIONS

The surface runoff, soil erosion, and percolation through a 1-m thick soil cover for the low-level radioactive waste disposal area at Los Alamos, MDA G, were simulated using a stochastic weather generator and a daily water balance model. Soil erosion was predicted using the MUSLE equation. A Monte Carlo approach was used that generated 100 realizations which were 10000 years long.

Precipitation parameters for the stochastic generator were estimated using data from the Los Alamos location rain gauge because the record for this site was longer. The mean annual precipitation was constrained to 35.56 cm which is the mean for the MDA G location from Bowen (1990). The seasonal distribution of the precipitation parameters from the White Rock gauge were compared to the Los Alamos gauge and the patterns were similar for the available data.

The simulated surface was a 1-m thick profile with a 10-cm layer of clayloam topsoil and the remaining depth composed of crushed tuff. Data from the stormwater runoff measuring stations at MDA G were available and the CN1 parameter was estimated from these data. Soil water characteristics and saturated hydraulic conductivity from a field experiment were used in place of soil texture based tabular values for the topsoil. Also, crushed tuff water characteristics were revised using data from MDA G.

Results from the base case simulation showed considerable variability in both percolation and surface runoff. The magnitude of the mean annual surface runoff is low compared with the available data from MDA G. Soil erosion is directly related to surface runoff through the MUSLE equation so the amount of soil erosion is low too. There was considerable variability in the percolation and surface runoff response which is essentially the same as the variability calculated by Springer (1995). Better estimates of key parameters such as soil water characteristics and CN1 did not reduce the uncertainty. Much of the uncertainty enters through the weather input.

The models and parameter values reflect the current appraisal of the lumped system at MDA G. Data such as chloride profiles, stable isotope distributions, and surface runoff are being collected, and these will provide some further constraints on future simulations. Also, MDA G will be closed and no further maintenance will be performed putting this system into an ecological and soil succession process. Parameters that control the hydrology will change with the succession process, but the pattern and magnitude of the change are unknown and not considered in this simulation study.

The following recommendations are made based on the results of this simulation study:

- Continue to collect soil moisture, chloride profile, and stable isotope data to constrain model parameters or replace model inputs. It may be possible to use the chloride profile data to estimate the subsurface flux rate.

- Implement a dynamic model that incorporates changes in vegetation and soil properties over time is needed.

- Consider implementing an event-based surface runoff model to account for the effects of high intensity rainfall events on runoff and erosion and the spatial distribution of soil properties. The current daily water balance model can be used for interstorm periods to predict antecedent conditions. This is expected to be more important for the soil erosion.

REFERENCES

Abeele, W. V. 1984. Geotechnical aspects of Hackroy sandy loam and crushed tuff. Los Alamos National Lab. Report No. LA-9916-MS, 20 pp.

Abeele, W. V., H. R. Fuentes, and J. Hosch. 1986. Characterization of soil moisture characteristic curves in the 30 to 1000 kPa tension range for Bandelier Tuff in waste disposal areas G and L, Technical Area 54, Los Alamos National Laboratory. Report prepared for Environmental Surveillance Group, HSE-8, Los Alamos National Laboratory, Los Alamos, NM, 99pp.

Abeele, W. V., M. L. Wheeler, and B. W. Burton. 1981. Geohydrology of Bandelier Tuff. Los Alamos Nat. Lab. Rep. No. LA-8962-MS, 50 pp.

Anderson, E. A. 1973. National Weather Service river forecast system -- snow accumulation and ablation model. NOAA Tech. Memo. NWS HYDRO-17, U.S. Dept. of Commerce, Silver Spring, MD, 217 pp.

Bowen, B. M. 1990. Los Alamos climatology. Los Alamos National Lab. Report No. LA-11735-MS, 254 pp.

Cooley, K. R., E. P. Springer, and A. L. Huber. 1987. Part I. Chapter 4. Hydrology component: snowmelt. Pages 31-40 in J. R. Wight and J. W. Skiles (eds.). SPUR - Simulation of Production and Utilization on Rangelands: Documentation and user guide. U.S. Department of Agriculture, Agricultural Research Service. ARS-63, 367 pp.

Haan, C. T. 1977. Statistical methods in hydrology. Iowa State Univ. Press, Ames, Iowa, 378 pp.

Hanson, C. L., and C. W. Richardson. 1987. Parameter estimation for the climate generator. Pages 300-320 in SPUR: Simulation of Production and Utilization of Rangelands. Documentation and user guide, J. R. Wight and J. W. Skiles, eds. U.S. Department of Agriculture, Agricultural Research Service, ARS 63, 372 pp.

Jackson, R. D., S. B. Idso and R. J. Reginato. 1976. Calculation of evaporation rates during the transition for energy-limiting to soil-limiting phases using albedo data. Water Resources Research 12(1):23-26.

Knisel, W. G. 1980. CREAMS: A field-scale model for Chemicals, Runoff, and Erosion from Agricultural Management Systems. USDA Conservation Res. Rep. No. 26, 643 pp.

Lane, L. J. 1984. Surface water management: A user's guide to calculate a water balance using the CREAMS model. Los Alamos National Laboratory Report No. LA-10177-MS, 49 pp.

Lane, L. J. and J. J. Stone. 1983. Water balance calculations, water use efficiency and aboveground net production. Pages 27-34 in Hydrology and water resources in Arizona and the southwest, Volume 13.

Lane, L. J., and V. A. Ferreira. 1980. Sensitivity analysis. Pages 113-158 in CREAMS: A field scale model for Chemicals, Runoff, and Erosion from Agricultural Management Systems, W. G. Knisel, ed. USDA Conservation Res. Rep. No. 26, 643 pp.

Lee, R. 1963. Evaluation of solar beam irradiation as a climatic parameter of mountain watersheds. Colo. State University Hydrology Papers, No. 2 (August 1963), Ft. Collins.

Link, S. O., L. L. Cadwell, K. L. Petersen, M. R. Sackschewsky, and D. S. Landeen. 1995. The role of plants and animals in isolation barriers at Hanford, Washington. Pacific Northwest Laboratory Report No. PNL-10788, Pacific Northwest laboratory, Richland, WA.

Matalas, N. C. 1967. Mathematical assessment of synthetic hydrology. Water Resources Research 3(4):937-945.

Newman, B. D. 1996. Vadose zone water movement at Area G, Los Alamos National Laboratory, TA-54: Interpretations based on chloride and stable isotope profiles. Los Alamos National Laboratory Report, LA-UR-96-4682, Los Alamos National Laboratory, Los Alamos, NM, 30pp.

Nyhan, J. W., W. V. Abeele, T. E. Hakonson, and E. A. Lopez. 1986. Technology development for the design of waste repositories at arid sites: Field studies of biointrusion and capillary barriers. Los Alamos National Laboratory Rep. No. LA-10574-MS, Los Alamos National Laboratory, Los Alamos, New Mexico, 50 pp.

Nyhan, J. W., R. Beckman, and B. Bowen. 1989. An analysis of precipitation occurrences in Los Alamos, New Mexico, for long-term predictions of waste repository behavior. Los Alamos National Laboratory Rep. No. LA-11459-MS, Los Alamos National Laboratory, Los Alamos, New Mexico, 27 pp.

Nyhan, J. W., G. L. Depoorter, B. J. Drennon, J. R. Simanton, and G. R. Foster. 1984. Erosion of earth covers used in shallow land burial al Los Alamos, New Mexico. J. Environmental Quality, 13(3):361-366.

Nyhan, J. W., L. W. Hacker, T. E. Calhoun, and D. L. Young. 1978. Soil survey of Los Alamos County, New Mexico. Los Alamos Report LA-6779-MS, Los Alamos National Laboratory, Los Alamos, New Mexico, 102 pp.

Nyhan, J. W., T. E Hakonson and B. J. Drennon. 1990. A water balance study of two landfill cover designs for semiarid regions. J. Environmental Quality, 19:281- 288.

Nyhan, J. W. and L. J. Lane. 1986a. Rainfall simulator studies of earth covers used in shallow land burial at Los Alamos, New Mexico. Pagers 39-42 in Proceedings of the Rainfall Simulator Workshop, January 14-15, 1985, Tucson, AZ, Society for Range management, Denver, CO.

Nyhan, J. W., and L. J. Lane. 1986b. Erosion control technology: A user's guide to the use of the Universal Soil Loss Equation at waste burial facilities. Los Alamos Report LA-10262-MS, Los Alamos National Laboratory, Los Alamos, New Mexico, 67 pp.

Renard, K. G., E. D. Shirley, J. R. Williams, and A. D. Nicks. 1987. Part I. Chapter 3. Hydrology component: Upland phases. Pages 17-30 in J. R. Wight and J. W. Skiles (eds.). SPUR - Simulation of Production and Utilization on Rangelands: Documentation and user guide. U.S. Department of Agriculture, Agricultural Research Service. ARS-63., 367 pp.

Richardson, C. W. 1982a. A comparison of three distributions for the generation of daily rainfall amounts, p. 67-78. In Singh, V.P., ed., Statistical Analysis of Rainfall and Runoff. Proceedings of International Symposium on Rainfall-Runoff Modeling, Water Research Publication, 700 p.

Richardson, C. W. 1982b. Dependence structure of daily temperature and solar radiation. Trans. ASAE, 25:735-739.

Richardson, C. W., C. L. Hanson, and A. L. Huber. 1987. Climate generator. Pages 3-16 in SPUR: Simulation of Production and Utilization of Rangelands. Documentation and user guide, J.R. Wight and J.W. Skiles, eds. U.S. Department of Agriculture, Agricultural Research Service, ARS 63, 372 pp.

Ritchie, J. T. 1972. A model for predicting evaporation from a row crop with incomplete cover. Water Resour. Res. 8:1204-1213.

Rogers, D. M. and B. M. Gallaher. 1995. The unsaturated hydraulic characteristics of Bandelier Tuff. Los Alamos National Laboratory Report, LA-12968-MS, Los Alamos National Laboratory, Los Alamos, NM, 132p.

Rogers, M. A. 1977. History and environmental setting of LASL near-surface land disposal facilities for radioactive wastes (Areas A, B, C, D, E, F, G, and T). Los Alamos Scientific Laboratory Rep., LA-6848-MS, Vol. 1.

Sejkora, K. J. and A. W. Alldredge. 1989. Influence of pocket gophers on water erosion and surface hydrology. Final report submitted to Los Alamos National Laboratory by Colorado State University, Department of Fish and Wildlife Biology, Fort Collins, CO, 144pp.

Springer, E. P. 1995. Area G performance assessment: Surface water and erosion. Los Alamos National Laboratory Report No., LA-UR-95-2497, Los Alamos National Laboratory, Los Alamos, NM, 40pp.

Springer, E. P., and L. J. Lane. 1987. Hydrology-component parameter estimation. Pages 260-275 in SPUR: Simulation of Production and Utilization of Rangelands. Documentation and user guide, J.R. Wight and J.W. Skiles, eds. U. S. Department of Agriculture, Agricultural Research Service, ARS 63, 372 pp.

Springer, E. P., B. J. McGurk, R. H. Hawkins, and G. B. Coltharp. 1980. Curve numbers from watershed data. In Watershed Management 1980, p. 938-950. Am. Soc. Civil Engin. Symposium on Watershed Management, Boise, Idaho.

Suter II, G. W., R. J. Luxmoore, and E. D. Smith. 1993. Compacted soil barriers at abandoned landfill sites are likely to fail in the long term. J. Environmental Quality, 22:217-226.

USDA, Soil Conservation Service. 1972. National engineering handbook, hydrology section 4, chapters 4-10.

van Genuchten, M. Th. 1980: A closed form equation for predicting the hydraulic conductivity of unsaturated soil. Soil Science Soc. Am. J. 44:892-898.

van Genuchten, M. Th., F. J. Leij, and S. R. Yates. 1991. The RETC code for quantifying the hydraulic functions of unsaturated soils. U. S. Environmental Protection Agency Rep. No. EPA/600/2-91/065, 85pp.

van Genuchten, M. Th., J. C. Parker, and J. B. Kool. 1987. Analysis and prediction of water and solute transport in a large lysimeter. Pages 4-36 in Modeling Study of Solute Transport in the Unsaturated Zone, Workshop proceedings. U. S. Nuclear Regulatory Comm., Washington, D.C., NUREG/CR-4615 vol. 2, 242 pp.

Warren, R.W., T. E. Hakonson, and K. V. Bostick. 1996. The hydrologic evaluation of four cover designs for hazardous waste landfills at Hill Air Force Base. Federal Facilities Environment Journal, Winter 1995/96, 91- 110.

Wight, J. R. and J. W. Skiles, eds. 1987. SPUR: Simulation of Production and Utilization of Rangelands. Documentation and user guide. U. S. Department of Agriculture, Agricultural Research Service, ARS 63, 372 pp.

Williams, J. R. and W. V. LaSeur. 1976. Water yield model using SCS curve numbers. Journal of the Hydraulics Division, American Society of Civil Engineers, 102(HY9):1241-1253.

Williams, J. R. 1975. Sediment yield prediction with universal equation using runoff energy factor. USDA, Agricultural Res. Service, ARS-S-40, pp. 244-252.

Wischmeier, W. H. and D. D. Smith. 1978. Predicting rainfall erosion losses -A guide to conservation planning. USDA Handbook 537, 58pp.

Woolhiser, D. A., R. E. Smith, and D. C. Goodrich. 1990. KINEROS, A kinematic runoff and erosion model: Documentation and user manual. U. S. Department of Agriculture, Agriculture Research Service, ARS-77, 130pp.